

Article

Preparation and Characterization of Intrinsic Low- κ Polyimide Films

Yu Sun, Tao Li *, Haiyang Dai, Manman Wang, Renzhong Xue, Jing Chen and Dewei Liu

Henan Key Laboratory of Magneto-electronic Information Functional Materials, College of Physics and Electronic Engineering, Zhengzhou University of Light Industry, Zhengzhou 450002, China; sy3115@126.com (Y.S.); daihaiyang720@163.com (H.D.); wmanman1@163.com (M.W.); xrbzbotao@163.com (R.X.); wulicj@126.com (J.C.); liudw2002@163.com (D.L.)

* Correspondence: taoli@zzuli.edu.cn

Abstract: Three fluorinated polyimide (PI-FP, PI-FO and PI-FH) films with low dielectric constants and excellent comprehensive properties were successfully prepared using a polycondensation reaction method by incorporating p-phenylenediamine (PDA), 4,4'-diaminodiphenyl ether (ODA) and 4,4'-(Hexafluoroisopropylidene) bis (p-phenyleneoxy) dianiline (HFPBDA) into 4,4'-(Hexafluoroisopropylidene) diphthalic anhydride (6FDA), respectively. The effects of the diamine monomer structure on optical, dielectric and mechanical properties were investigated. Compared with PDA and ODA, HFPBDA can effectively improve the optical and dielectric properties of PI due to its special chain structure. Among the three PI films, PI-FH film presents the best optical transmission (highest transmittance = 90.2%) and highest energy gap (2.69 eV). The dielectric properties of PI-FH film improve the most. The dielectric constant and loss at 10^4 Hz are reduced to 2.05 and 0.0034 at 10^4 Hz, respectively, and remain stable up to 250 °C. The mechanical properties decrease in turn for PI-FP, PI-FO and PI-FH films due to the increase in free volume fraction. Nevertheless, PI-FH film still exhibits good mechanical properties with a tensile strength of 88.4 Mpa, a tensile modulus of 2.11 GPa and an elongation at break of 4.1%. The correlation between the dielectric and mechanical properties of PI films and their free volume characteristics is well explained with the help of positron annihilation spectroscopy.

Keywords: polyimide; low dielectric constants; positron annihilation; free volume fraction



Citation: Sun, Y.; Li, T.; Dai, H.; Wang, M.; Xue, R.; Chen, J.; Liu, D. Preparation and Characterization of Intrinsic Low- κ Polyimide Films. *Polymers* **2021**, *13*, 4174. <https://doi.org/10.3390/polym13234174>

Academic Editor: Alexey V. Lyulin

Received: 31 October 2021

Accepted: 26 November 2021

Published: 29 November 2021

Publisher's Note: MDPI stays neutral with regard to jurisdictional claims in published maps and institutional affiliations.



Copyright: © 2021 by the authors. Licensee MDPI, Basel, Switzerland. This article is an open access article distributed under the terms and conditions of the Creative Commons Attribution (CC BY) license (<https://creativecommons.org/licenses/by/4.0/>).

1. Introduction

With the rapid development of the integration level for ultralarge-scale integration (ULSI) in the semiconductor industry, the size of electronic devices is reducing and the density of transistors is increasing, causing an increase in interconnection delays, cross-talk noise and the power dissipation of circuits [1–4]. It has become a bottleneck restricting further improvements in the speed of integrated circuits, mainly because the dielectric performance of traditional low dielectric material (SiO_2) between lines in microelectronic circuits cannot meet the requirements for the dielectric constant (k) = 3.9–4.2. Studies show that [5–7] some materials with ultra-low k are used to replace traditional low-dielectric SiO_2 , which can effectively reduce the interconnection delay, crosstalk and energy consumption. Therefore, in the context of the deep development of ULSI, the development and application of high-performance dielectric materials with low dielectric ($k \leq 2.5$) and ultra-low dielectric ($k \leq 2.0$) constants is urgent and inevitable. Such dielectric materials as interlayer dielectrics can reduce the capacitance between the metal interconnections, the resistance capacitance delay, the line-to-line crosstalk noise, and the power dissipation [8,9]. In recent years, polymer materials are considered as a kind of low dielectric materials with good application prospects in ULSI due to their natural low density, good flexibility, low molecular polarizability and natural microporosity. Among these polymer materials, polyimide (PI) films attracted more attention and are widely used as electronic materials

due to their low dielectric constants, and good thermal and chemical stability; therefore, they are currently considered as one of the most promising polymer candidates for the next generation of high-performance interlayer dielectrics in microelectronic devices [10–12]. However, traditional PIs, such as commercial DuPont Kapton PI films, have a k value of 3.2–3.8 [13], which struggles to meet the requirement of ultra-low k (≤ 2.0) for ULSI. Hence, it is significant and urgent to develop new PIs with ultra-low dielectric constants. Many experimental methods are used to reduce the dielectric constant of PIs. Introducing pores can effectively reduce the k values and was successfully used to create ultra-low- k , accompanied by a loss of the mechanical strength of PIs [5,14–17]. Therefore, researchers propose designing an appropriate molecular structure to equip low- k PIs with low dielectric constants without damaging their excellent intrinsic properties. Fluorine atoms have high electronegativity, which can reduce the conjugation of electron clouds in the molecular structure, in turn reducing the molecular polarizability. Therefore, introducing fluorine atoms into the main chain and increasing fluorine content to prepare PI films with low k values is widely reported [3,8,18–21]. However, studies show that there are some limitations in reducing the k value of polyimide only by increasing the fluorine content. When k decreases to 2.4, the further decrease in k is not clear with the increasing fluorine content [22]. At the same time, with the increase in fluorine content, the hydrogen fluoride generated at a high temperature causes more serious corrosion to inorganic materials [23], and the adhesion and mechanical strength of materials weaken to a certain extent. In addition, substituent group with large volume can hinder the dense stacking of molecular chains, then increase the free volume fraction of polymers, thus reducing the number of polarized molecules per unit volume [24,25]. Therefore, diamines or dianhydride with macromolecular groups are often used to synthesize PIs with low dielectric constant.

Positron annihilation spectroscopy, as a means of solid defect detection [26], was widely used in the study of defects (including defect vacancies, dislocations, vacancy clusters, holes, etc.) in metals, semiconductors, ceramics and other materials. In porous materials, a fraction of the positrons injected from the positron source formed positronium, which was annihilated from the para state (p -Ps, singlet spin state) by emitting two γ -rays with a lifetime of ~ 125 ps or annihilated from the ortho state (o -Ps, triplet spin state) by emitting three γ -rays, with a lifetime 142 ns (in a vacuum environment). The formation probability for p -Ps and o -Ps is 1:3. The o -Ps will pick off one electron from the surrounding molecules and annihilate with a typical value of 1–5 ns in local free volumes, due to collisions with molecules. The pick-off annihilation lifetime of o -Ps is highly sensitive to the size of the pores. The o -Ps can accurately detect the ultra-micropores because the size of o -Ps is only 1.06 Å, much smaller than that of all gas molecules. In addition, positron annihilation spectroscopy is not limited by open or closed pores, which is a powerful means to study porous polymer materials, and played a huge role in the study of free volume pores and pore structure in polymers [27].

In this work, tree fluorinated PI films were prepared by polycondensation reaction using 6FDA as the dianhydride monomer, and PDA, ODA, and HFPBDA as the diamine monomer, respectively. The effects of diamine monomer structure on optical, dielectric and mechanical properties were investigated. The correlation between the dielectric and mechanical properties of PI films and their free volume characteristics was well explained with the help of unique experimental probes such as positron annihilation spectroscopy.

2. Materials and Methods

2.1. Materials and PI Film Fabrication

6FDA (99%), PDA (99%), ODA (98%), HFBAPP (97%) and *N,N*-Dimethyl- form amide (DMF) ($\geq 99.9\%$) were bought from Aladdin Industrial Corporation (Shanghai, China). A certain proportional amount of diamine (PDA, ODA or HFPBDA) in proportion was weighed according to the solid content of 15% and dissolved in 20 mL DMF in a dried 50 mL flask filled with argon. After the diamine was completely dissolved, 6FDA were weighed in proportion and added into the diamine solution. Then, the flask was put into

the ice water mixture, and the magnetic stirrer was used to stir the solution for 8 h, after the polymerization, a viscous, homogeneous, transparent, light-yellow polyamic acid (PAA) solution was obtained. The synthesis reaction process and the photos of the PI films are shown in Figure 1. Finally, after coating on to clean glass plates, the PPA solution was heated at 300 °C for 2 h under vacuum to thoroughly remove the solvent. Three kinds of PI films were thus obtained and the thickness measured ranged from 0.019–0.021 nm. The films were coded PI-FP, PI-FO and PI-FH, where PI-FP represented 6FDA-PDA, PI-FO represented 6FDA-ODA and PI-FH represented 6FDA- HFPBDA, respectively.

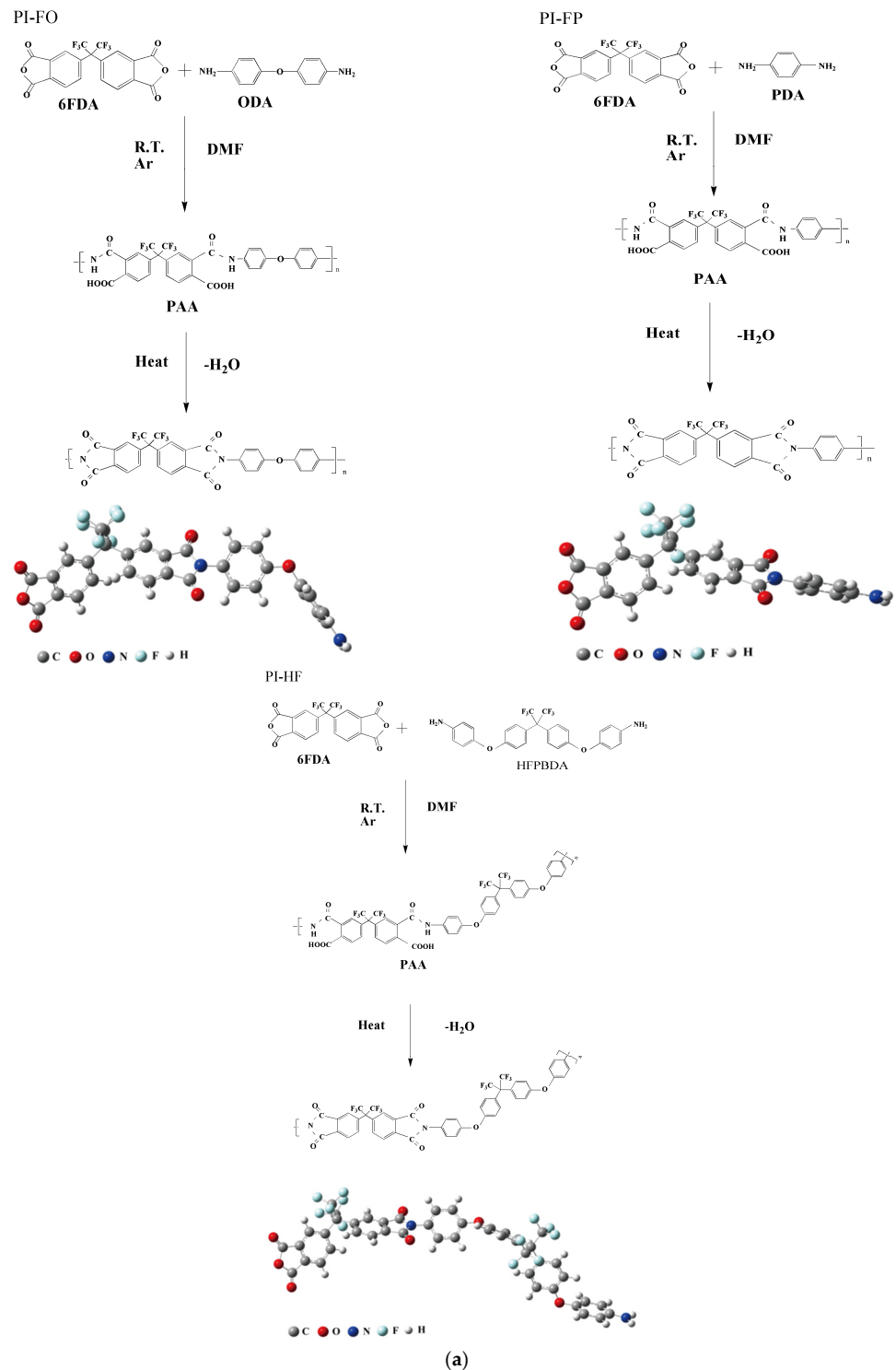


Figure 1. Cont.

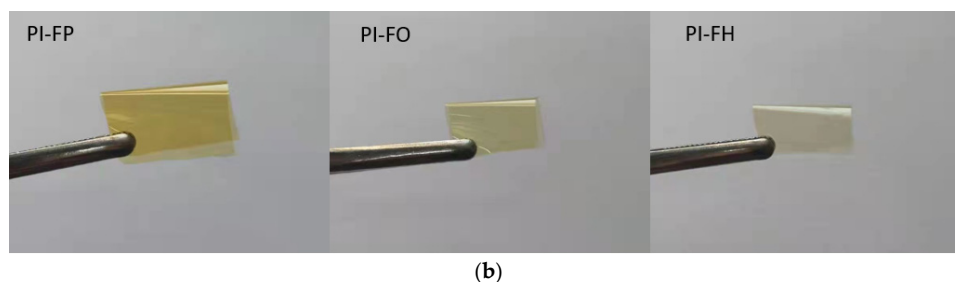


Figure 1. The synthesis procedure for PPA (a) and the photos of the PI films (b).

2.2. Characterization

The microstructures were characterized by flourier transform infrared spectroscopy (FT-IR) spectra recorded in the transmittance mode on a spectrometer (VERTEX70, Bruker Company, Rudolf-Plank-Str. 27. Ettlingen, Germany). Positron annihilation lifetime spectra were measured using a conventional fast-fast coincidence lifetime spectrometer (Ortec Company, Oak Ridge, TN, USA) with a time resolution of 220 ps and a channel width of 13.0 ps. A ^{22}Na positron source with the activity of $\sim 20 \mu\text{Ci}$ sealed between Kapton films was sandwiched between two identical samples (The superposition thickness of PI films on each side of positron source is about 1 mm.) measurements and each spectrum contains more than 1.5×10^6 counts and the obtained lifetime spectra were resolved using PATFIT software package. The transmittance spectra of Ultraviolet-visible for PI films in the wavelength range of 200–800 nm were measured using a UV-VIA-NIR (UH4150, Hitachi Company, 6-6, Marunouchi 1-chome, Chiyoda-ku, Tokyo, Japan) spectrometer. The dielectric properties of the PI films were determined using an Agilent 4294A Precision Impedance Analyzer and Dielectric temperature spectrum measurement system (DMS2000, Partulab company, No. 602, building 9, Guanggu New Power Industrial Park, Gaoxin Road 5, Donghu New Technology Development Zone, Jiangxia District, Wuhan, China). The k value was calculated according to the equation: $k = \frac{Cd}{k_0S}$, where C is the capacitance value, k_0 is the dielectric constant of vacuum which is $8.85 \times 10^{-12} \text{ F/m}$; S and d are the electrode area and thickness of the films. The electric breakdown properties were tested by Voltage-dependent Resistor Characteristic (HG2516, Changzhou Yangzi Electronic Comany, Qingyang Road 2, Xinbei District, Changzhou, China), and the mechanical properties by an electronic universal test machine (UTM 2202, Shenzhen Suns Technology Stock Company, Heli Road 5, Shenzhen, China), and the deformation rate in tensile tests is 10 mm/min.

3. Results and Discussion

3.1. FT-IR Spectra and EDX

FT-IR spectra of PI films are presented in Figure 2. All of the PI films show characteristic imide absorption peaks, which are consistent with the results reported in the relevant studies [11,12,21]. The peak at 725 cm^{-1} represents the bending vibration of $\text{C}=\text{O}$ in the imide ring. The peak at 1376 cm^{-1} represents the stretching vibration of $\text{C}-\text{N}$ in the imide ring. The peaks at 1719 cm^{-1} and 1774 cm^{-1} represent the symmetrical stretching vibrations and the asymmetrical carbonyl stretching vibrations of $\text{C}=\text{O}$, respectively, in the imide ring. The peak at 1510 cm^{-1} represents the stretching vibration peak of the ben-zene ring, and the peak at 3072 cm^{-1} represents the stretching vibration of $\text{C}-\text{H}$ on the benzene ring. The FT-IR spectra results indicate the successful reaction between the dia-mine monomers (PDA, ODA and HFPBDA) and the dianhydride (6FDA), as well as the complete imidization reaction of PAA. In addition, the $\text{C}-\text{F}$ stretch vibration absorption peak from the trifluoromethyl ($-\text{CF}_3$) groups is observed near 1150 cm^{-1} (within the pink dotted line), and the absorption intensity of PI-FH is much stronger than that of PI-FP and PI-OP due to more $-\text{CF}_3$ groups in the molecular chain unit of PI-FH. The EDX results of PI films are shown in Figure 3; it can be seen that the F element content is 21.94 wt%, 20.26 wt% and 32.14 wt% for PI-FP, PI-FO and PI-FH, respectively.

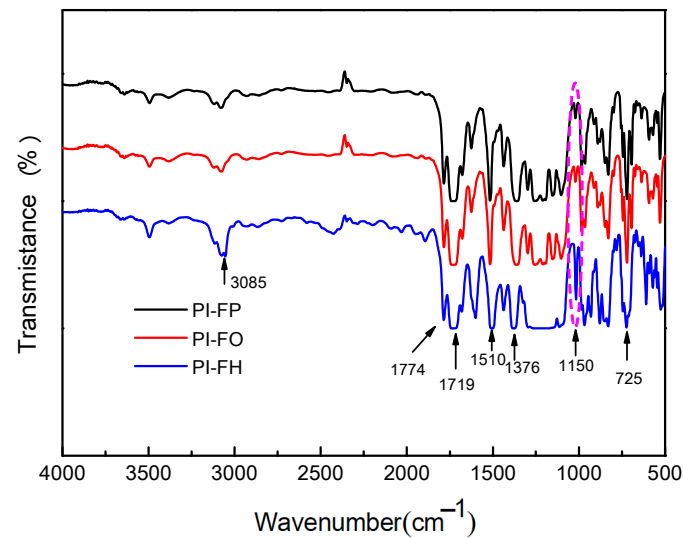


Figure 2. FT—R spectra of PI films.

3.2. Positron Annihilation Analysis

The discrete analysis method is widely used to analyze the positron lifetime spectrum. In this analysis, the ideal positron lifetime $L(t)$ is the superposition of multiple exponential positron components, which can be expressed by the following formula [28]:

$$L(t) = \sum_{i=1}^n I_i \exp(-t\lambda_i) \quad (1)$$

where n is the number of components; I_i is the initial intensity of component I ; t is time(channel number); λ_i is the annihilation rate of component I , whose reciprocal ($1/\lambda_i$) is the average life τ_i of component I . In the actual measurement, considering the time resolution of the instrument, the positron lifetime spectrum ($Y(t)$) obtained becomes the convolution of the ideal lifetime spectrum and the instrument resolution function:

$$Y(t) = L(t) \cdot R(t) = N_t \sum_{i=1}^n I_i \int_0^{\infty} R(t-t') \exp(-\lambda_i t') dt' + B \quad (2)$$

where N_t and B are the total count and the background count of life spectrum; $R(t)$ is the resolution function of the lifetime spectrometer; $R(t) = \frac{1}{\sigma\sqrt{\pi}} e^{-\left(\frac{t}{\sigma}\right)^2}$, $\sigma = \frac{FWHM}{2\sqrt{2}}$, σ is standard deviation; and $FWHM$ is full width at half maximum of the Gaussian function. Based on Equation (2), the positron lifetime spectrum can be fitted by the least square method to obtain λ_i and I_i . At present, PATFIT is a widely used spectrum resolution software package, in which POSITRONFIT can be used to obtain the lifetime τ_i and its intensity I_i .

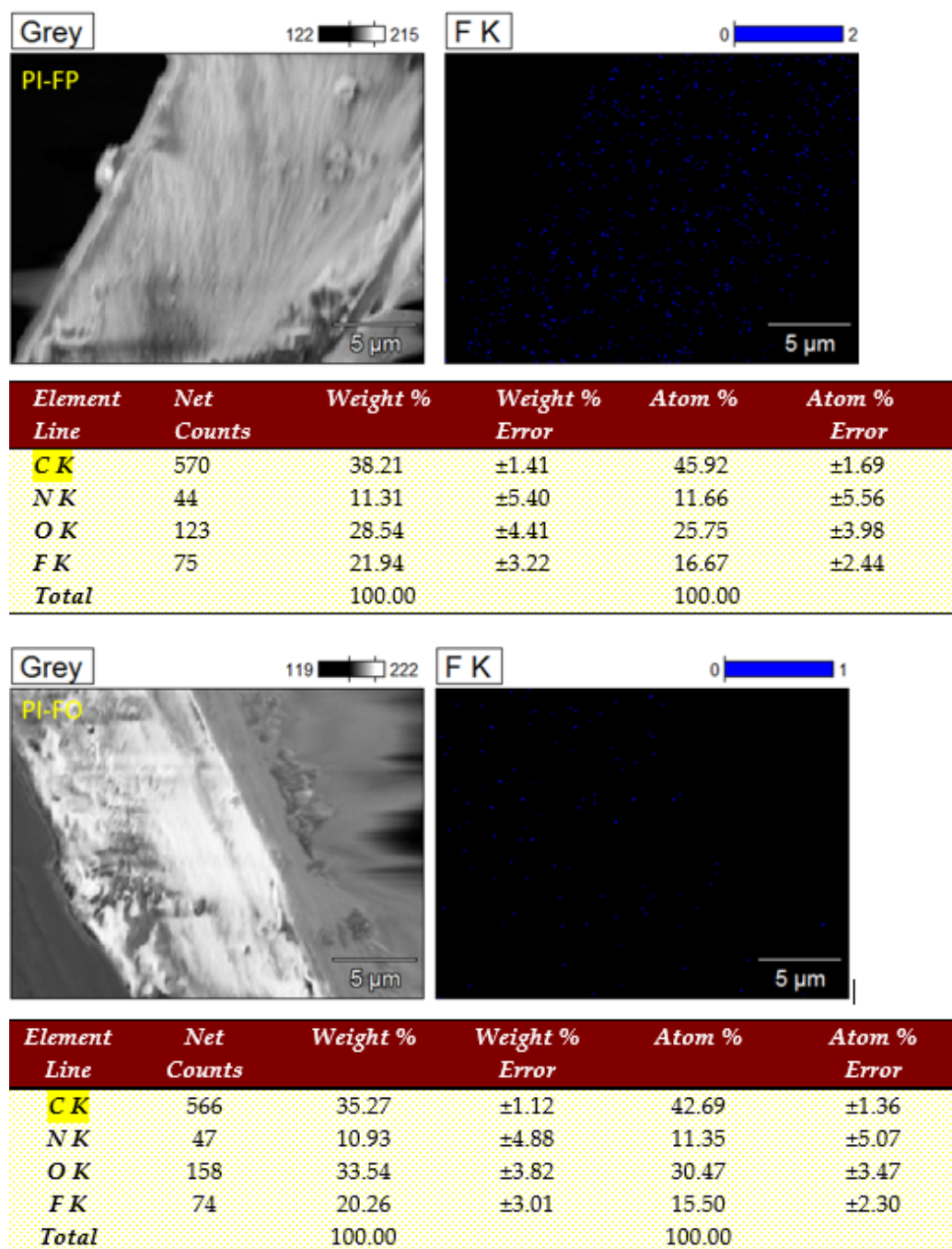


Figure 3. Cont.

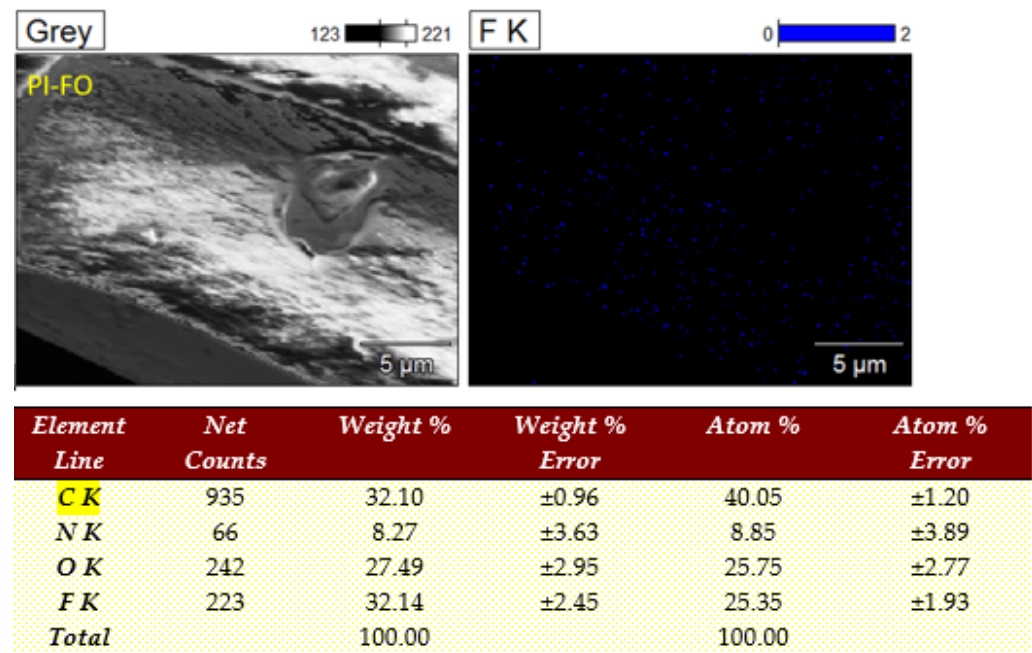


Figure 3. EDX of PI films.

The positron lifetime spectra for PI films are shown in Figure 4 and the detailed positron life time parameters are listed in Table 1, in which there are three lifetime components (τ_1 , τ_2 and τ_3) and their corresponding intensities (I_1 , I_2 and I_3) for PI-FP, PI-FO and PI-FH films, respectively. The τ_1 is derived from the *p*-Ps lifetime and the free annihilation lifetime of the positrons. The τ_2 (424–444 ps) is due to the annihilation of free positrons trapped in vacancy-type defects on the polymer chains or free volume defects (cavities or vacancies or low-electron-density sections) of PI films without forming the metastable bound state, i.e., Ps. The τ_3 in the range of 2031 ps to 2246 ps corresponds to the pick-off annihilation of *o*-Ps in the free volume of the amorphous phase for the PI films [27,29]. The probability of the pick-off annihilation of *o*-Ps is related to the size of the free volume. Therefore, the lifetime of *o*-Ps is also directly related to the size of free volume that can be estimated by the Tao-Eldrup model [30]:

$$\tau_3 = 0.5ns \left[1 - \frac{R}{R + \Delta R} + \frac{1}{2\pi} \sin \left(\frac{2\pi R}{R + \Delta R} \right) \right]^{-1} \quad (3)$$

where τ_3 is the annihilation lifetime of *o*-Ps; the prefactor of 0.5 ns is the spin-averaged Ps annihilation lifetime, which is also observed in densely packed molecular crystals [8]; R is the radius of voids; ΔR is the empirical electron layer thickness parameter around the voids, normally taken as 0.1656 nm. The intensity (I_3) of the *o*-Ps pick-off annihilation is closely related to the free volume fraction of polymer. The free volume fractional FFV_{PALS} can be estimated by the semi-empirical equation [31]:

$$FFV_{PALS} = CV_f I_3 \quad (4)$$

where C is a material-dependent constant which is defined as 0.0018 \AA^{-3} [31–33]; $V_f = \frac{4}{3}\pi R^3$; I_3 is the intensities of τ_3 . The free volume parameters of the PI films calculated according to Equations (3) and (4) are given in Table 2. The free volume fraction of PI-OP is almost the same as that of PI-FP. However, that of the PI-FH film is significantly higher than that of the former two films.

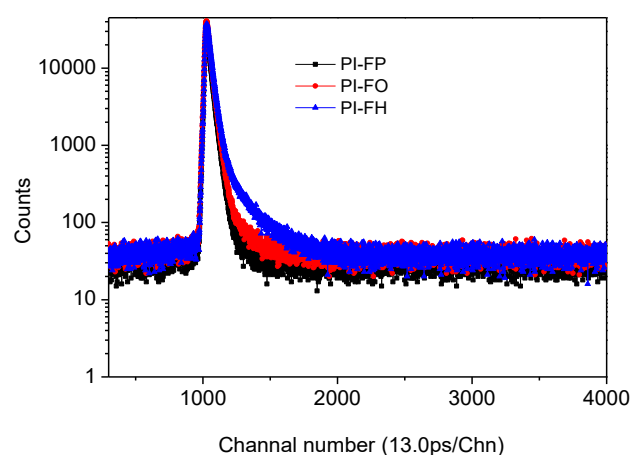


Figure 4. Positron life spectrum of the PI films.

Table 1. The positron life time parameters of PI films.

PI Films	τ_1/ps	τ_2/ps	τ_3/ps	$I_1/\%$	$I_2/\%$	$I_3/\%$
PI-FP	210.5 ± 4.6	429.6 ± 3.7	2031.4 ± 30.3	36.4 ± 2.3	58.6 ± 2.1	5.0 ± 0.6
PI-FO	220.6 ± 5.4	424.6 ± 3.5	2059.3 ± 28.2	32.7 ± 1.4	61.0 ± 1.3	5.9 ± 0.8
PI-FH	225.4 ± 9.0	444.9 ± 9.2	2246.2 ± 29.9	30.6 ± 3.6	59.7 ± 3.5	9.7 ± 1.4

Table 2. The free volume hole parameters of PI films.

PI Films	$R/\text{Å}$	$V_f/\text{Å}^3$	$f_r/\%$
PI-FP	2.88 ± 0.02	99.76 ± 2.83	0.90 ± 0.02
PI-FO	2.90 ± 0.03	102.39 ± 2.68	1.09 ± 0.02
PI-FH	3.06 ± 0.02	120.48 ± 2.96	2.10 ± 0.04

The characteristics of the free volume defect are closely related to the molecular chain structure. The calculated results of free volume parameters for the three PI films indicate that the chain length of molecular units and the number of $-\text{CF}_3$ groups in the molecular chain unit have a significant effect on the free volume size and the free volume fraction of polyimide. A long molecular chain unit with more benzene rings can inhibit the dense stacking of molecular chain because the adjacent benzene rings form a non-coplanar structure due to the repulsion between the π bonds. In addition, the $-\text{CF}_3$ group with large molar volumes can also effectively inhibit the dense stacking of molecular chain. Therefore, PI-FH has a longer molecular chain unit and more $-\text{CF}_3$ groups than the other two PIs, which makes PI-FH film have a larger free volume size and higher free volume fraction than other two PI films.

3.3. UV-Visible Transmission Spectra

The UV-VIS transmittance spectra in the range of $400\text{--}650\text{ nm}^{-1}$ of PI-FP, PI-FO and PI-FH are shown in Figure 5, and their highest transmittance is shown in Table 3. The transmittance increase in turn for the three PI films and accordingly, the color gradually fades from orange to light yellow (Figure 1b). In general, the UV-Vis transmittance and coloration of aromatic polymers depends on the formation of their charge transfer complexation (CTC) and/or conjugated aromatic structures [34]. The $-\text{CF}_3$ has a negative effect on the conjugation degree of aromatic structure. The fluorine atoms with strong ability of electron-withdrawing can inhibit the formation of the intermolecular and intramolecular CTC and increase the transmittance of PI [35].

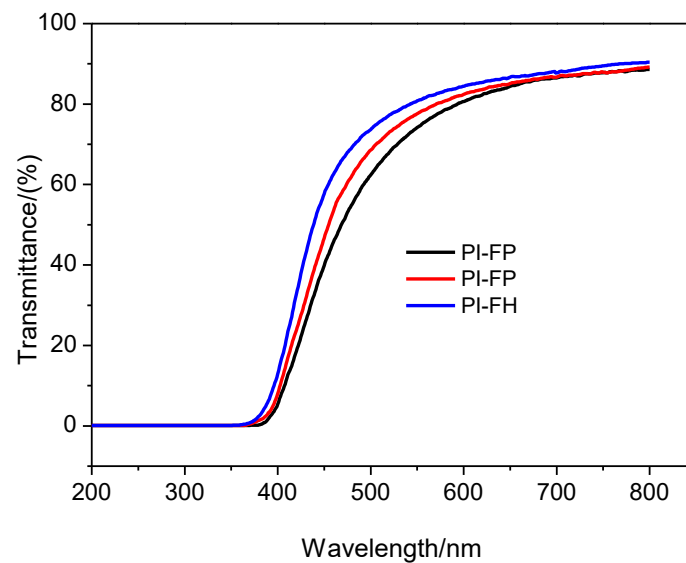


Figure 5. UV–VIS transmittance spectra of the PI films.

Table 3. The cut-off wavelength and highest transmittance of PI films.

Films	Highest Transmittance/%	E_g /eV
PI-FP	88.5 ± 2.0	2.56
PI-FO	88.8 ± 2.3	2.58
PI-FH	90.2 ± 2.1	2.69

In addition, the energy gap (E_g) is an important optical parameter, which can be obtained (according to Figure 6) by Equation (5):

$$\left(\frac{\alpha h\nu}{K}\right)^{1/2} = h\nu - E_g \quad (5)$$

where α is the absorption coefficient, which can be obtained in terms of: $\alpha = (1/d) \ln(1/T)$, d is the film thickness, T is the transmission, K is a coefficient, h is the Planck constant, and ν is the photon frequency. The E_g value can be obtained based on the linear approximation of the absorption edge to the energy axis, i.e., the intercept at the energy axis. The estimated E_g value is 2.56 eV, 2.58 eV and 2.69 eV for PI-FP, PI-FO and PI-FH films, respectively.

The effect of the conjugation degree of the aromatic structure on the optical property of the polymer can be determined by the energy gap, since the length of conjugation within the polymer chain is related to the E_g . The $-\text{CF}_3$ group with a large volume located on the side of the polymer chain leads to the torsion of molecular chains and reduces conjugation length in the molecular chain, thus reducing the conjugation absorption. In addition, the oxyether ($-\text{O}-$) bond can break the conjugation of the molecular chain and weaken the large π conjugation absorption of the aromatic polymer chain. Therefore, the increase in the number of $-\text{CF}_3$ groups and oxygen ether bonds in the molecular chain can lead to the increase in E_g .

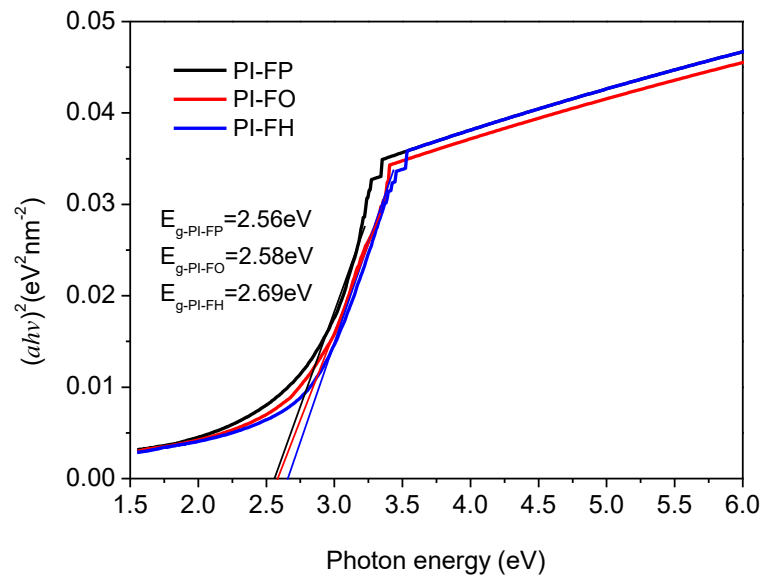


Figure 6. The relation between absorption coefficient spectra and the energy gap.

3.4. Dielectric Properties

The dependence of the dielectric properties on the frequencies of PI films at room temperature is shown in Figure 7, and the measured dielectric constant dielectric loss at 10^4 Hz is listed in Table 4. The films exhibit low dielectric constants (k) of 2.06–2.92 at 10^4 Hz, which are much lower than the dielectric constant of a commercial PI film (3.49 at 10^4 Hz). The dielectric constant of PI-FO is only slightly lower than that of PI-FP. However, the dielectric constant of PI-FH film is much lower than that of the former two films.

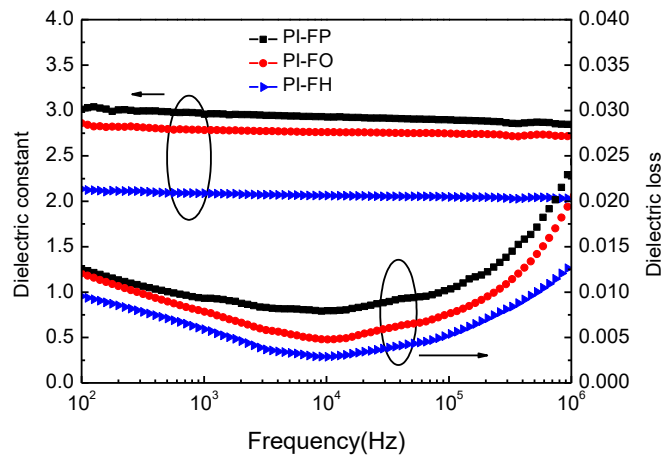


Figure 7. The dependence of the dielectric properties on frequency for PI films at room temperature.

Table 4. The dielectric parameters of PI films.

Films	$k/10$ kHz	$D/10$ kHz (10^{-2})	Electrical Breakdown (kV/mm)
PI-FP	2.92 ± 0.08	0.83 ± 0.03	65.4 ± 2.8
PI-FO	2.76 ± 0.07	0.52 ± 0.03	61.3 ± 2.5
PI-FH	2.05 ± 0.07	0.34 ± 0.03	51.6 ± 2.1

The dielectric constant mainly depends on the number of polarized molecules per unit volume of polymer [26,36]. The relation between the dielectric constant and polarizability can be explained by the Debye equation [21].

$$\frac{k-1}{k+2} = \frac{4}{3}\pi N \left(a_e + a_d + \frac{\mu^2}{3k_b T} \right) \quad (6)$$

where k is dielectric constant, N is the number density of dipoles, a_e the electric polarization, a_d is the distortion polarization, μ is the orientation polarization related to the dipole moment, and T and k_b are temperature and the Boltzmann constant, respectively.

The influence of $-\text{CF}_3$ groups located at the side molecular chain on the dielectric properties of PI includes two aspects. On the one hand, $-\text{CF}_3$ groups can hinder the dense stacking behavior of molecular chains, increase the free volume fraction, and then reduce the number of polarized molecules (N) per unit volume. On the other hand, less bond-conjugated electrons can lead to the reduction in a_e , a_d and μ due to the strong ability of the electron-withdrawing of fluorine atoms [21]. The free volume fraction of PI-FO is slightly higher than that of PI-FP, resulting in a higher dielectric constant of PI-FO than that of PI-FP. Compared with PI-FP and PI-FO films, the PI-FP film presents the lowest dielectric constant ($k = 2.05$) due to the most $-\text{CF}_3$ groups contained in the molecular chain units of PI-FP. According to the definition of ultra-low dielectric constant (≤ 2.0) material, the PI-FP film can be approximately regarded as an ultra-low dielectric PI film.

In addition, low dielectric loss (D) is an important index to evaluate the dielectric properties of dielectric materials. Generally, the total energy loss in dielectric materials including the loss from the dielectric relaxation process and loss from DC conductivity can be expressed as Equation (7) [37]:

$$D = \frac{\omega^2 \varepsilon_0 \tau (\varepsilon'_s - \varepsilon'_\alpha) + (1 + \omega^2 \tau^2) \sigma_{dc}}{\omega \varepsilon_0 (\varepsilon'_s + \varepsilon'_\alpha \omega^2 \tau^2)} \quad (7)$$

where ω is the frequency; ε'_s and ε'_α are the static and high-frequency permittivity; τ is relaxation time of the polarized molecule; ε_0 is permittivity of the vacuum; and σ_{dc} is DC conductivity. At low frequencies, $\omega\tau \ll 1$, the dielectric loss mainly dominated by σ_{dc} and at high frequencies, $\sigma_{dc} = 0$, the dielectric loss mainly dominated by τ . The high free volume fraction is conducive reducing σ_{dc} , and then reducing the dielectric loss from leakage conduction at low frequencies. The low molecular polarizability is conducive to reduce the dielectric loss at high frequencies from the relaxation of polarization molecular. Therefore, the high free volume fraction and low molecular polarizability are beneficial to reduce the dielectric loss of polymers [38]. PI-FP has extremely low dielectric loss values ($D = 0.0034$) at 10^4 Hz, which are very important for reducing the energy consumption of devices when applied as an interlayer medium applied in ULSI. The temperature dependence of the dielectric properties at 10^4 Hz for the three PI films is shown in Figure 8. All the curves of the dielectric constant and loss versus temperature display a very good stability of up to 250°C . The excellent temperature stability of dielectric properties suggests a good potential for microelectronic applications as dielectric and insulating materials.

The electrical breakdown strength is an important parameter to evaluate the insulating performance of dielectric materials. Because breakdown strength can lead to a short circuit which seriously damages the electronic devices. The measured DC breakdown strength values of the three PI films are shown in Table 4. The breakdown strength decreases successively, which can be ascribed to the gradual increase in the average size of free volume and the fraction of free volume for PI-FP, PI-FO and PI-FH films.

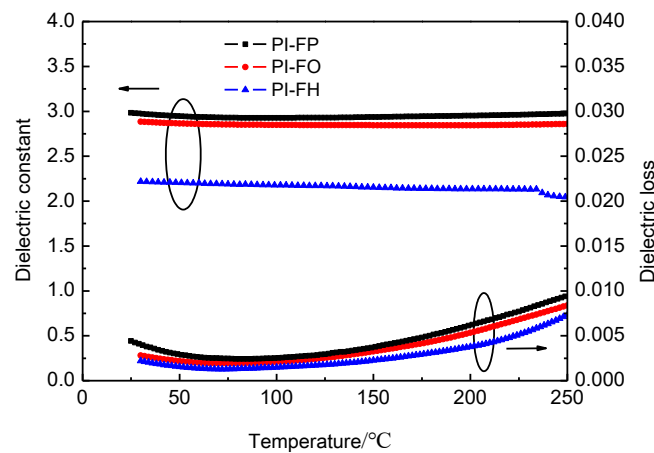


Figure 8. The temperature dependence of the dielectric properties at 10^4 Hz for PI films.

3.5. Mechanical Properties

The mechanical property of the PI-based film is identified as an important index to evaluate its application as an interlayer material. The measured stress-strain curves of films subjected to tensile tests at room temperature are displayed in Figure 9. The measured tensile strength, tensile modulus, and elongation at break of films are listed in Table 5. The tensile strength decreases gradually from 122.5 MPa for the PI-FP film, to 109.6 MPa for PI-FO film, and to 88.4 MPa for PI-FH film. Accordingly, the tensile modulus decreases gradually from 2.86 GPa for the PI-FP film, to 2.42 GPa for PI-FO film, and to 2.11 GPa for PI-FH film; the elongation at break decreases from 5.1% for the PI-FP film, to 4.6% for the PI-FO film and to 4.1% for the PI-FH film. Generally, the mechanical properties of polymers are affected by many factors, such as free volume defect, structure of molecular chain, crystallinity, test temperature and so on. Firstly, the free volume factor is very important. It is considered that the tensile strength of the PI film decreases with the increase in free volume size and free volume fraction [29]. Secondly, the molecular chain structure cannot be ignored. When the $-\text{CF}_3$ groups are introduced into the molecule chain, the electron cloud of the C-C bond will transfer to the side of the C atom close to $-\text{CF}_3$ due to the strong electron-withdrawing ability of fluorine atoms, which reduces the bond energy of C-C bond, and then reduces the tensile strength. In addition, the bond energy of C-O (326 kJ/mol) is slightly lower than that of C-C (332 kJ/mol), which is the reason in the decline of mechanical properties of PI-FO compared with PI-FP. Therefore, according to the free volume parameters and the structure of molecular chain units of the three PI films, it is not difficult to understand that the mechanical properties decrease in turn for PI-FP, PI-FO, and PI-FH films. In addition, the existence of an -O- bond in the molecular chain increases the flexibility of the molecular chain and reduces the tensile modulus of the PI film [25]. Therefore, the tensile modulus decreases in turn for PI-FP, PI-FO, and PI-FH films. Nevertheless, it is worth noting that the PI-FH film still exhibits good mechanical properties compared with the other fluorinated PI films, as reported in studies [20,39] on the case of excellent dielectric properties (Figure 9).

Table 5. The tensile strength, tensile modulus, and elongation at break of PI films.

Films	Tensile Strength/MPa	Tensile Modulus/GPa	Elongation at Break (%)
PI-FP	122.5 ± 3.7	2.86 ± 0.08	5.1 ± 1.4
PI-FO	109.6 ± 3.4	2.42 ± 0.07	4.6 ± 1.2
PI-FH	88.4 ± 3.1	2.11 ± 0.05	4.1 ± 0.9

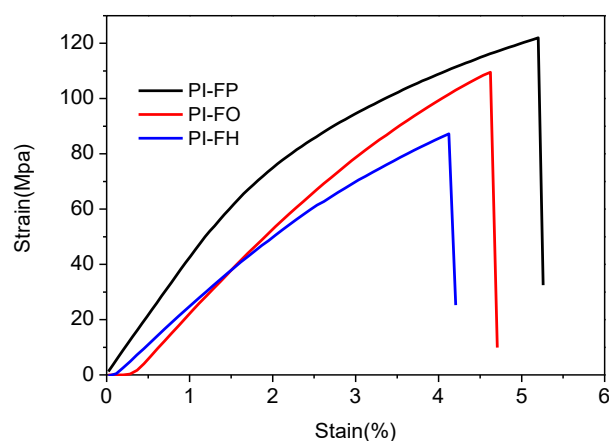


Figure 9. Measured stress versus strain curves of PI films subjected to tensile tests.

4. Conclusions

In summary, three PI films were synthesized by means of polycondensation, taking 6FDA, PDA, ODA and HFPBDA as raw materials. The optical and dielectric properties of PI film were improved by changing of diamine monomer structure. Among the three PI films, the PI-FH film presents the best optic transmission (highest transmittance = 90.2%) and the best dielectric properties ($k = 2.05$, $D = 0.0034$ at 10^4 Hz). Compared with PDA and ODA residues, HFPBDA residue has more $-CF_3$ groups and a longer chain length. The $-CF_3$ groups can effectively weaken the intermolecular and intramolecular CTC effect and the conjugation degree of the aromatic structure, and then increase the optic transmission and energy gap. Compared with PDA and ODA residues, the HFPBDA residue in the molecular chain can more effectively increase the free volume fraction of PI, and then reduce the number of polarized molecules per unit volume. Additionally, the $-CF_3$ can reduce the polarizability due to the strong electron-withdrawing ability of fluorine atoms. This is the main reason that the dielectric properties of PI-FH film are the most improved. The mechanical properties weaken in turn for PI-FP, PI-PO and PI-FH films. Nevertheless, the PI-FH film still exhibits a tensile strength of 88.4 Mpa at room temperature considering its excellent dielectric properties. This study establishes a novel method of understanding the dielectric and mechanical properties of PI films based on their free volume defect characteristics and the correlation between them, aided by positron annihilation spectroscopy.

Author Contributions: Data curation, Y.S.; Project administration, Conceptualization, Writing—original draft, Writing—review & editing, T.L.; Formal analysis, H.D.; Investigation, M.W.; Funding acquisition, R.X.; Supervision, J.C.; Visualization, D.L. All authors have read and agreed to the published version of the manuscript.

Funding: This study is supported by the National Natural Science Foundation of China (Project No. 11975211, 11775192, 12005194) and Key Research and Development and promotion projects in Henan Province (Project No. 212102210485, 212102210132, 202102210489), as well as by Postgraduate Education Reform and Quality Improvement Projects in Henan Province (No. HNYJS2021AL027).

Institutional Review Board Statement: Not applicable.

Informed Consent Statement: Not applicable.

Data Availability Statement: Not applicable.

Conflicts of Interest: The authors declare no conflict of interest.

References

1. Lee, Y.J.; Huang, J.M.; Kuo, S.W.; Chang, F.C. Low-dielectric, nanoporous polyimide films prepared from PEO-POSS nanoparticles. *Polymer* **2005**, *46*, 10056–10065. [[CrossRef](#)]
2. Volksen, W.; Miller, R.D.; Dubois, G. Low dielectric constant materials. *Chem. Rev.* **2010**, *110*, 56–110. [[CrossRef](#)]
3. Yuan, C.; Jin, K.K.; Li, K.; Diao, S.; Tong, J.W.; Fang, Q. Non-porous low-k dielectric films based on a new structural amorphous fluoropolymer. *Adv. Mater.* **2013**, *25*, 4875–4878. [[CrossRef](#)] [[PubMed](#)]
4. Tong, J.W.; Diao, S.; Jin, K.K.; Yuan, C.; Wang, J.J.; Sun, J.; Fang, Q. Benzocyclobutene-functionalized poly(m-phenylene): A novel polymer with low dielectric constant and high thermostability. *Polymer* **2014**, *55*, 3628–3633. [[CrossRef](#)]
5. Zhou, H.; Wei, D.Y.; Fan, Y.; Chen, H.; Yang, Y.S.; Yu, J.J.; Jin, L.G. Dielectric properties of polyimide/SiO₂ hollow spheres composite films with ultralow dielectric constant. *Mat. Sci. Eng. Chem.* **2016**, *203*, 13–18. [[CrossRef](#)]
6. Liu, X.X.; Li, Y.P.; Guo, W.M.; Sun, X.N.; Feng, Y.; Sun, D.; Liu, Y.Y.; Yan, K.; Wu, Z.H.; Su, B.; et al. Dielectric and mechanical properties of polyimide composite films reinforced with graphene nanoribbon. *Surf. Coat. Tech.* **2017**, *320*, 497–502. [[CrossRef](#)]
7. Yang, K.S.; Kang, Y.Y.; Ahn, H.J.; Kim, D.G.; Park, N.K.; Choi, S.Y.Q.; Won, J.C.; Kim, Y.H. Porous boron nitride/polyimide composite films with high thermal diffusivity and low dielectric properties via high internal phase Pickering emulsion method. *J. Ind. Eng. Chem.* **2020**, *82*, 173–179. [[CrossRef](#)]
8. Liu, Y.W.; Qian, C.; Qu, L.J.; Wu, Y.; Zhang, Y.; Wu, X.H.; Zou, B.; Chen, W.X.; Chen, Z.Q.; Chi, Z.G.; et al. A bulk dielectric polymer film with intrinsic ultralow dielectric constant and outstanding comprehensive properties. *Chem. Mater.* **2015**, *27*, 6543–6549. [[CrossRef](#)]
9. Huang, Y.W.; Wei, X.N.; Liu, L.L.; Yu, H.T.; Yang, J.X. A novel pore-free strategy via interfacial effects in nanocomposites to produce polyethylene with ultra-low dielectric constants. *Mater. Lett.* **2018**, *232*, 86–91. [[CrossRef](#)]
10. Cao, K.; Yang, L.; Huang, Y.W.; Chang, G.J.; Yang, J.X. High temperature thermosets derived from benzocyclobutene-containing main-chain oligomeric carbosilanes. *Polymer* **2014**, *55*, 5680–5688. [[CrossRef](#)]
11. Zhong, M.; Wu, X.M.; Shu, C.; Wang, Y.L.; Huang, X.Y.; Huang, W. Organosoluble polyimides with low dielectric constant prepared from an asymmetric diamine containing bulky *m*-trifluoromethyl phenyl group. *React. Funct. Polym.* **2021**, *169*, 05065. [[CrossRef](#)]
12. Wang, Z.Q.; Zhang, M.Y.; Han, E.L.; Niu, H.Q.; Wu, D.Z. Structure-property relationship of low dielectric constant polyimide fibers containing fluorine groups. *Polymer* **2020**, *206*, 122884. [[CrossRef](#)]
13. Popovici, D.; Hulubei, C.; Cozan, V.; Lisa, G.; Bruma, M. Polyimides containing cycloaliphatic segments for low dielectric material. *High Perform. Polym.* **2012**, *24*, 194–199. [[CrossRef](#)]
14. Ma, S.D.; Wang, Y.; Liu, C.; Xu, Q.; Min, Z.H. Preparation and characterization of nanoporous polyimide membrane by the template method as low-k dielectric material. *Polym. Adv. Technol.* **2016**, *27*, 414–418. [[CrossRef](#)]
15. Wang, Q.H.; Wang, C.; Wang, T. Controllable low dielectric porous polyimide films templated by silica microspheres: Microstructure, formation mechanism and properties. *J. Colloid Interface Sci.* **2013**, *389*, 99–105. [[CrossRef](#)]
16. Devaraju, S.; Vengatesan, M.R.; Selvi, M.; Kumar, A.A. Synthesis and characterization of bisphenol—A ether diamine-based polyimide POSS nanocomposites for low *k* dielectric and flame-retardant. *Appl. High Perform. Polym.* **2012**, *24*, 85–96. [[CrossRef](#)]
17. Othman, M.B.H.; Ramli, M.R.; Tyng, L.Y.; Ahmad, Z.; Akil, H.M. Dielectric constant and refractive index of poly (siloxane-imide) block copolymer. *Mater. Des.* **2011**, *32*, 3173–3182. [[CrossRef](#)]
18. Chen, Z.G.; Liu, S.M.; Yan, S.J.; Shu, X.; Yuan, Y.C.; Huang, H.H.; Zhao, J.Q. Overall improvement in dielectric and mechanical properties of porous graphene fluoroxide/polyimide nanocomposite films via bubble-stretching approach. *Mater. Des.* **2017**, *117*, 150–156. [[CrossRef](#)]
19. Ma, T.; Zhang, S.J.; Li, Y.; Li, F.; Yang, F.C.; Gong, C.L.; Zhao, J.J. Synthesis and characterization of soluble polyimides based on a new fluorinated diamine: 4-Phenyl-2,6-bis[3-(4'-amino-2'-trifluoromethyl-phenoxy)phenyl] pyridine. *J. Fluor. Chem.* **2010**, *131*, 724–730. [[CrossRef](#)]
20. Wu, T.T.; Dong, J.; Gan, F.; Fang, Y.; Zhao, X.; Zhang, Q. Low dielectric constant and moisture-resistant polyimide aerogels containing trifluoromethyl pendent groups. *Appl. Surf. Sci.* **2018**, *440*, 595–605. [[CrossRef](#)]
21. Wang, Z.H.; Fang, G.Q.; He, J.J.; Yang, H.X.; Yang, S.Y. Semi-aromatic thermosetting polyimide resins containing alicyclic units for achieving low melt viscosity and low dielectric constant. *React. Funct. Polym.* **2020**, *146*, 104411. [[CrossRef](#)]
22. Maier, G. Low dielectric constant polymers for microelectronics. *Prog. Polym. Sci.* **2001**, *26*, 3–65. [[CrossRef](#)]
23. Jin, Y.X.; Tang, J.; Hu, J.; Xan, X.; Shang, Y.Z.; Liu, H.L. One-step fabrication of ultralow dielectric polyimide films consisting of size-controlled mesoporous nanoparticles. *Colloids Surf. A* **2011**, *392*, 178–186. [[CrossRef](#)]
24. Yang, C.P.; Chiang, H.C.; Chen, K.H. Organosoluble and light-colored fluorinated polyimides based on 9,9-Bis[4-(4-amino-2-trifluoromethylphenoxy)phenyl]fluorene and aromatic dianhydrides. *Colloid Polym. Sci.* **2004**, *28*, 1347–1358. [[CrossRef](#)]
25. Liaw, D.J.; Wang, K.L.; Huang, Y.C.; Lee, K.R.; Lai, J.Y.; Ha, C.S. Advanced polyimide materials: Syntheses, physical properties and applications. *Prog. Polym. Sci.* **2012**, *37*, 907–974. [[CrossRef](#)]
26. Brusa, R.S.; Spagolla, M.; Karwasz, G.P.; Zecca, A. Porosity in low dielectric constant SiOCH films depth profiled by positron annihilation spectroscopy. *J. Appl. Phys.* **2004**, *95*, 2348. [[CrossRef](#)]
27. Zhao, Y.; Huang, R.; Wu, Z.; Zhang, H.; Zhou, Z.; Li, L.; Dong, Y.; Luo, M.; Ye, B.; Zhang, H. Effect of free volume on cryogenic mechanical properties of epoxy resin reinforced by hyperbranched polymers. *Mater. Des.* **2021**, *202*, 109565. [[CrossRef](#)]

28. Zhou, B.; Li, C.Y.; Qi, N.; Jiang, M.; Wang, B.; Chen, Z.Q. Pore structure of mesoporous silica (KIT-6) synthesized at different temperatures using positron as a nondestructive probe. *Appl. Surf. Sci.* **2018**, *450*, 31–37. [[CrossRef](#)]
29. Zhang, H.J.; Sellaiyan, S.; Kakizaki, T.; Uedono, A.; Taniguchi, Y.; Hayashi, K. Effect of freevolume holes on dynamic mechanical properties of epoxy resins for carbon-fiber-reinforced polymers. *Macromolecules* **2017**, *50*, 3933–3942. [[CrossRef](#)]
30. Eldrup, M.; Lightbody, D.; Sherwood, J.N. The temperature dependence of positron lifetimes in solid pivalic acid. *Chem. Phys.* **1981**, *63*, 51–58. [[CrossRef](#)]
31. Li, T.Y.; Liu, J.J.; Zhao, S.S.; Chen, Z.Q.; Huang, H.H.; Guo, R.L.; Chen, Y.M. Microporous polyimides containing bulky tetra-*o*-isopropyl and naphthalene groups for gas separation membranes. *J. Membr. Sci.* **2019**, *585*, 282–288. [[CrossRef](#)]
32. Ji, M.C.; Zhou, M.T.; Li, Y.J.; Lu, G.L.; Huang, X.Y. Construction of semi-fluorinated polyimides with perfluorocyclobutyl aryl ether-based side chains. *Polym. Chem.* **2018**, *9*, 920–930. [[CrossRef](#)]
33. Japip, S.; Lee, G.R.; Chung, T.S. The role of fluorinated aryl ether moiety in polyimide-co-etherimide on gas transport properties. *Ind. Eng. Chem. Res.* **2020**, *59*, 5315–5323. [[CrossRef](#)]
34. Khalil, M.; Saeed, S.; Ahmad, Z. Properties of binary polyimide blends containing hexafluoroisopropylidene group. *J. Macromol. Sci. A* **2006**, *44*, 55–63. [[CrossRef](#)]
35. Lee, C.K.; Shul, Y.G.; Han, H. Dielectric properties of oxydianiline-based polyimide thin films according to the water uptake. *J. Polym. Sci. Pol. Phys.* **2002**, *40*, 2190–2198. [[CrossRef](#)]
36. Liu, X.D.; Hou, Z.L.; Zhang, B.X.; Zhan, K.T.; He, P.; Zhang, K.L.; Song, W.L. A general model of dielectric constant for porous materials. *Appl. Phys. Lett.* **2016**, *108*, 102902. [[CrossRef](#)]
37. Vangchangyia, S.; Swatsitang, E.; Thongbai, P.; Pinitsoontorn, S.; Yamwong, T.; Maensiri, S.; Amornkitbamrung, V. Very low loss tangent and high dielectric permittivity in pure-CaCu₃Ti₄O₁₂ ceramics prepared by a modified sol-gel process. *J. Am. Ceram. Soc.* **2012**, *95*, 1497–1500. [[CrossRef](#)]
38. Fu, J.; Hou, Y.D.; Zheng, M.P.; Wei, Q.Y.; Zhu, M.K.; Yan, H. Improving dielectric properties of PVDF composites by employing surface modified strong polarized BaTiO₃ particles derived by molten salt method. *ACS Appl. Mater. Interfaces* **2015**, *44*, 24480–24491. [[CrossRef](#)]
39. Neyertz, S.; Brown, D.; Douanne, A.; Bas, C.; Albérola, N.D. The molecular structure and dynamics of short oligomers of PMDA-ODA and BCDA-ODA polyimides in the absence and presence of water. *J. Phys. Chem. B* **2002**, *106*, 4617–4631. [[CrossRef](#)]